Quantum Mechanical – NMR Aided Configuration and Conformation of Two Unreported Macrocycles Isolated from the Soft Coral *Lobophytum* sp. : Energy Calculations *vs* Coupling Constants

Song-Wei Li[§,¶,‡], Cristina Cuadrado[Δ,‡], Li-Gong Yao[§], Antonio Hernandez Daranas[Δ,*], Yue-Wei Guo[§,*]

[§] State Key Laboratory of Drug Research, Shanghai Institute of Materia Medica, Chinese Academy of Sciences, No. 555, Zu Chong Zhi Road, Zhangjiang Hi-Tech Park, Shanghai 201203, China

[¶] Nanjing University of Chinese Medicine, 138 Xianlin Road, Nanjing 210023, China

[Δ] Instituto de Productos Naturales y Agrobiología, Consejo Superior de Investigaciones Científicas (IPNA-CSIC), La Laguna, 38206 Tenerife, Spain

Supporting Information Placeholder

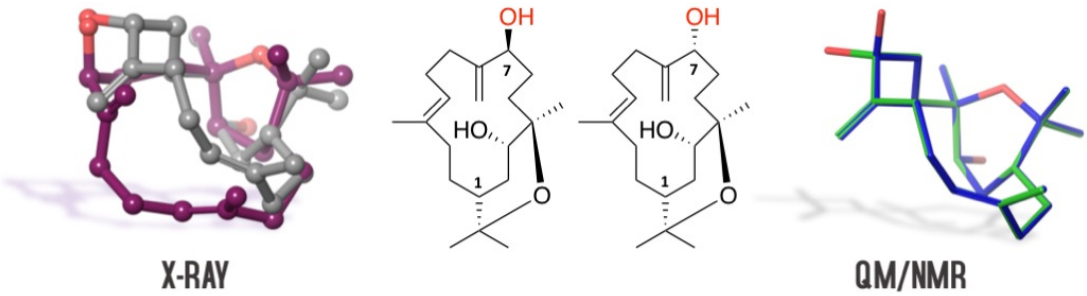

ABSTRACT: Two new macrocyclic cembranoids were isolated from the South China Sea soft coral *Lobophytum* sp. Quantum Mechanical – NMR methods were decisive in their structural elucidation. Better performance in arriving at definitive structures was obtained by QM-NMR methods incorporating $^{3}J_{HH}$ values. The validity of this approach also supported an alternative conformational proposal to that obtained by X-ray crystallography.

Marine benthic invertebrates produce an unparalleled variety of complex secondary metabolites with wide spectra of bioactivities.[1] In particular, soft corals of the genus *Lobophytum* exemplifies an intensive research subject and have been proved to be rich sources of structurally intriguing and biologically interesting secondary metabolites. Particularly cembranes are characteristic and dominant metabolites of *Lobophytum* and some of them showed promising biological activities, such as antitumoral, antiviral, anti-inflammatory, and neuroprotective.[2] An essential stage in the discovery of any new compound involves the accurate determination of its full structure. This is of extreme importance as it is strongly linked to its physical-chemical and biological properties. It may also have important consequences on intellectual property issues such as the CON201 case.[3] This task is particularly challenging in natural products chemistry so several erroneous structures are continually being detected and revised.[4-6] Despite NMR and X-ray crystallography are the gold-standard techniques used for structure elucidation, computational methods are gradually becoming a faster and sometimes even more reliable alternative.[7,8]

In our continuous effort to discover bioactive marine natural products from Chinese soft corals,[9-11] *Lobophytum* sp. was collected off the coast of Xisha Island, Hainan Province. Chemical investigation yielded two new cembranoids, namely lobophytolins A (**1**) and B (**2**), along with a known related one, isodecaryiol (**3**) (Figure 1). Their structures were elucidated by NMR spectroscopy, quantum chemical calculations, as well as X-ray diffraction analysis. The difficulties encountered for determining their full structures led us to use and compare different approaches. The results illustrate some caveats usually found in this task and tools that can be applied to unravel them.

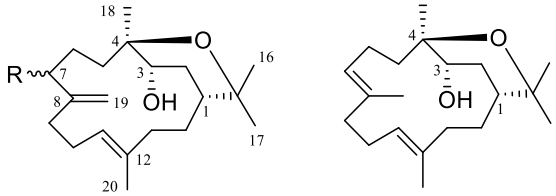

1 R = -OH
2 R = -OH

3

Figure 1. Structures of **1**–**3**.

The usual work-up[9-11] of the Et_2O-soluble portion of the acetone extract of *Lobophytum* sp. yielded the pure compounds **1** (6.0 mg), **2** (8.7 mg) and **3** (4.5 mg). Compound **3** was identified as isodecaryiol, a cembranoid previously isolated from the Madagascar soft coral *Sinularia gravis*,[12] by comparison of its spectral data with those previously reported.

Lobophytolin A (**1**) was obtained as colorless crystals with a melting point of 116-117 °C and $[\alpha]^{20}_{,D}$ + 44.1 (*c* 0.4, $CHCl_3$). A HR-ESIMS ion peak at *m/z* 345.2407 $[M+Na]^+$ (calcd. 345.2400) revealed a molecular formula of $C_{20}H_{34}O_3$. The ^1H and ^{13}C NMR spectroscopic data of **1** showed the presence of a trisubstituted olefin (δ_H 5.32, dd, *J* = 10.3, 5.1 Hz; δ_C 126.9, 134.2) and an exocyclic double bond (δ_H 5.13, s; 5.09, s; δ_C 108.1, 149.7). Thus, to complete the four degrees of unsaturation of its molecular formula, compound **1** has a bicyclic structure. Moreover, the presence of two oxygenated methines (δ_H 3.71, dd, *J* = 8.8, 2.8 Hz; δ_C 70.7; δ_H 4.24, dd, *J* = 6.0, 4.0 Hz; δ_C 74.0), two non-protonated oxygenated carbon atoms (δ_C 76.3 and 75.8) and four singlets methyls suggested that **1** was closely related to isodecaryiol.[12] Analysis of 2D NMR data enabled structure elucidation of **1**. Thus, a COSY experiment led to the identification of three ^1H-^1H spin systems (Figure 2). These fragments were interconnected by analysis of long-range ^1H-^{13}C correlations obtained from the HMBC experiment. Particularly important were the large number of connectivities observed for methyl groups and their vicinal non-protonated carbons.

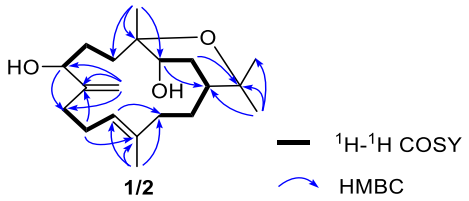

Figure 2. Key COSY and HMBC correlations of **1** and **2**.

Lobophytolin B (**2**) was obtained as colorless crystals with melting point of 132-133 °C and $[\alpha]^{20}_{,D}$ + 38.7 (*c* 0.2, $CHCl_3$). Its molecular formula was deduced as $C_{20}H_{34}O_3$ by HR-ESIMS from the ion peak at *m/z* 321.2435 $[M-H]^-$ (calcd. 321.2435), the same as that of **1**. Analysis of ^1H and ^{13}C NMR data showed that **2** was very similar to **1** (Table 1, SI). The main difference was observed at C-7 (δ_C 74.0 for **1** *versus* 78.4 for **2**), suggesting that **2** was simply the C-7 epimer of **1**. Further analysis of 2D NMR spectra confirmed this hypothesis.

Once the planar structures of **1** and **2** were elucidated, determination of their stereochemical features was undertaken. The configuration of the double bond $\Delta^{11,12}$ was assigned as *E* on the basis of the observed dipolar correlations between H11 and H13 as well as between methyl 20 and H10. A tentative relative configuration of the three asymmetric centers located within the oxane ring was built from the similarity of their NMR chemical shifts with **3**. Chemical shift overlapping (H1 and H2) prevented measurements of $^3J_{HH}$ or an unambiguous analysis of the NOESY experiment. Another major difficulty was to connect the relative configuration of the oxane ring with the remote position C7. This kind of problem has been tackled using *J*-based conformational analysis (JBCA) and/or NOESY analysis.[13-15] However, in the present case both stereoclusters are separated by non-protonated atoms (C4), which precludes the use of JBCA. The assignment based exclusively on dipolar correlations is usually uncertain in conformationally flexible molecules such as macrocycles.

Continuous advances in computation have made quantum mechanical methods one of the most popular strategies to face structural problems, by calculating spectroscopic properties. Currently, this approach is widely used to find the most likely structure from among a set of putative candidates.[16,17] In particular, NMR chemical shifts calculations have been used to address complex stereochemical problems by comparing experimental and computed values.[18] Dedicated metrics have been recently developed for this task. Among these, the DP4 probability stands out from all the others.[19] It was articulated on the basis that Bayes' theorem can be used to estimate the probability that the selected structure is the correct one. Improved versions such as DP4.2, DP4+ and the J-DP4 methods have been developed.[20-22]

Therefore, to define the relative configurations of compounds **1** and **2**, theoretical calculations of NMR parameters were used. First of all, conformational searches on the eight possible candidate diasteroisomers were done. To keep the computational cost to a minimum, a 12 kJ mol^{-1} energy cut-off was used, following previous reports that have shown that larger values don't give significant improvement but come with greater computational cost.[19] Afterwards, geometrical optimization at the DFT level were undertaken using the B3LYP functional with the 6-31G* basis set. Next, NMR calculations were carried out at the PCM/mPW1PW91/6-31+G** level, as recommended for DP4+. NMR shielding constants were calculated using the GIAO approach. Finally, shielding constants were averaged over the Boltzmann distribution obtained for each stereoisomer and correlated with the experimental data. The previous calculations gave conclusive guidance on the relative configuration at C1, C3 and C4, whereas the configuration at C-7 could not be irrefutably determined. This was not unexpected given the separation of the two stereoclusters. In addition, we speculated that the modest reproduction of the experimental NMR trends could be due to the choice of using a low energy-cutoff during the conformational search, which could have caused losing potentially relevant conformations. Similar situations have been previously described from a sequential one-by-one comparison between experimental data for each compound and all set of computed data.[23] It has been suggested that comparing all sets of experimental and predicted data simultaneously may give better results in these situations. However, in practice it is very uncommon to have the full set of experimental values for all possible stereoisomers, to be compared with all candidate structures.[24,25]

In our opinion, one important source of error in those methods based upon comparison between experimental NMR chemical shifts and their quantum mechanical prediction is related to the limited ability of theoretical calculations to appropriately represent the real conformational distribution of the studied molecule. For instance, a small relative error of ±1 kcal mol^{-1} in the free energy difference between two conformations changes their relative population from 7:3 to 3:7. Therefore, it is a general trend that potentially flexible molecules with complex energy landscapes give lower quality predictions.

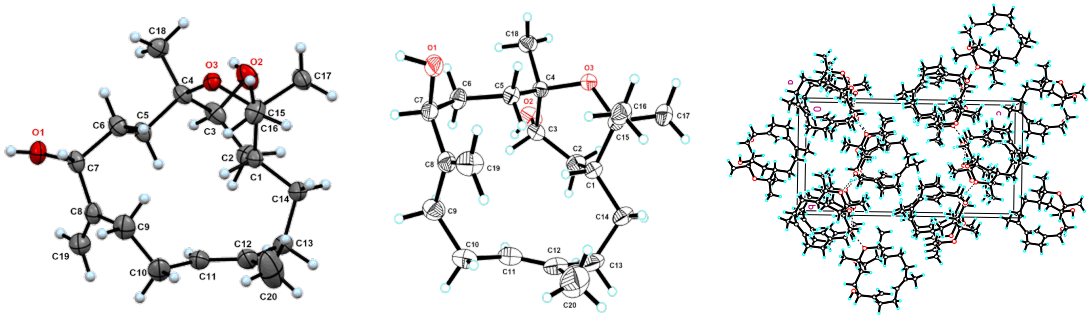

Figure 3. X-ray crystallographic structures of **1** (left), **2** (middle) and a fragment of the crystal packing of **2** (right)

Alternatively, readily available $^3J_{HH}$ measurements provide extremely valuable information in this context as they can amend the effect on the calculations of including wrong conformations.[22,26] In consequence, we used the recently developed i*J*/d*J*-DP4 protocol that includes J_{HH} values to constrain the conformational sampling problem. It has been shown that this solves the previous drawback, at least in part. Thus, we performed NMR calculations at the B3LYP/6-31G**//MMFF level of theory validated for this method. $^3J_{HH}$ values were computed considering only the Fermi contact term as recommended, then used to create a subset of candidates compatible with experimental measurements (i*J*-DP4 step). Because the structural changes were located around C7, only H7 coupling constants were used in this step. A difference cut-off of 2.5 Hz from the experimental value was used for such task. Finally, using only the selected compatible conformations (table S5) we proceeded with the analysis, now making use of all $^3J_{HH}$ and chemical shift values (d*J*-DP4 step). For methylene protons, the calculated $^3J_{HH}$ - chemical shift pairs were kept together and arranged against the experimental values using $^3J_{HH}$ as the leading value. By means of this approach, it turned out that the experimentally observed NMR data for compound **1** gave the best match of over 99% with isomer 1*R*,3*S*,4*R*,7*R*. On the other hand, the comparison using the NMR experimental data for compound **2** gave its best match for isomer1*R*,3*S*,4*R*,7*S*, with a 99 % probability. Despite most $^3J_{HH}$ experimental values were similar, the different coupling constant values measured for H7 in **1** (dd, J = 6.0, 4.0 Hz) and **2** (dd, J = 10.3, 4.0 Hz) turned out to be decisive to discriminate them.

To confirm the previous proposal, the absolute configuration of **1** was unequivocally confirmed as 1*R*,3*S*,4*R*,7*R* by X-ray crystal diffraction analysis using Ga Kα radiation (λ = 1.34139 Å), showing a low Flack parameter of -0.01 (13) (Figure 3). Likewise, the absolute configuration of **2** was determined to be 1*R*,3*S*,4*R*,7*S* by X-ray crystal diffraction using Cu Kα radiation (λ = 1.54178 Å), showing a Flack parameter of 0.30 (15) (Figure 3). Our previous stereochemical proposal based on the i*J*/d*J*-DP4 calculations neatly matched the crystallographic structures in both cases. However, the difference between the conformations of the two crystallographic structures was surprising. This was unexpected because the experimental NMR chemical shifts and $^3J_{HH}$ values of both compounds were very similar (excluding the C7 position and surroundings).

At this point, it is worth mentioning that the crystallographic structure of **1** (shown in gray in Figure 4) is different from the lowest energy conformation found in our calculations (shown in orange in Figure 4). This theoretical structure was removed from the analysis in the i*J*-DP4 step of our calculations, as it was not compatible with the available $^3J_{HH}$ measurements. From this, the second lowest energy conformation (shown in green in Figure 4, and almost superimposable with the crystallographic structure) emerged as the structure most likely to be fully compatible with NMR data. This situation may explain how i*J*/d*J*-DP4 found the right answer for this structure.

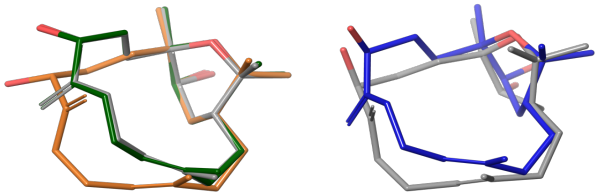

Figure 4. On the left, structures of **1**: X-ray structure (Gray), lowest energy conformer (Orange), 2nd lowest energy conformer (Green). On the right, structures of **2**: X-ray structure (Gray), lowest energy conformer (Blue).

The situation with compound **2** was different, since its crystallographic structure was not fully compatible with experimental $^3J_{HH}$. Moreover, the lowest energy conformation found in our calculations (shown in blue in Figure 4) was different from the X-ray structure but compatible with $^3J_{HH}$ values. A closer look at the crystal packing of **2** suggests that this situation may be a consequence of an intermolecular H-bond formed between the hydroxyl group at C7 and the ether oxygen atom, a situation that does not seem to occur in solution (Figure 3). Additionally, the computed structure (shown in blue in Figure 4) predicted by the i*J*/d*J*-DP4 protocol closely resembles that found for compound **1**, in accordance with the experimental NMR data available. In consequence, we regard the later as the conformation in $CDCl_3$ solution.

As an additional test, a DP4+ analysis was done using only the X-ray structures. The NMR experimental data of both compounds pointed to the 7*R* isomer (**1**). From our perspective, the later result arises from the fact that the calculations chose the "appropriate" conformation in solution, that comes only from the 7*R* epimer (**1**).

Compounds **1**–**3** were tested for cytotoxicity. All were found inactive at the concentration of 10 μM, on the tumor cell lines of HT-29, Capan-1, A549, and SNU-398. Interestingly, despite their structural similarity, **2** showed IC_{50} values ranging from 30 to 40 μM while **1** showed no activity within the tested concentrations (>50 μM).

The structure elucidation of lobophytolins A and B reveals some of the potential drawbacks faced in flexible molecules when following QM/NMR approaches. These methods rely heavily on the calculation of relative energies to predict the necessary Boltzmann weighting factors. However, the current limitations of DFT methods generate important errors whenever those energies are poorly predicted or when conformational sampling is not adequate. To correct this, alternative solutions such as the creation of random ensembles or the incorporation of structural information obtained from easily available $^3J_{HH}$ have been proposed.[22,27] Thus, using i*J*/d*J*-DP4 method we have successfully elucidated two macrocyclic structures and simultaneously found a conformational proposal in solution. The latter suggests that the solution and solid-state conformations of **2** are different.

ASSOCIATED CONTENT

Supporting Information

The Supporting Information is available free of charge on the ACS Publications website.

Experimental details, IR, MS and NMR spectra for all compounds, as well as computational details, coordinate files, experimental and calculated NMR data, correlation plots and values for DP4+ and *J*-DP4 methods (PDF)

AUTHOR INFORMATION

Corresponding Authors

Yue-Wei Guo - *State Key Laboratory of Drug Research, Shanghai Institute of Materia Medica, Chinese Academy of Sciences, No. 555, Zu Chong Zhi Road, Zhangjiang Hi-Tech Park, Shanghai 201203, China;* Email: ywguo@simm.ac.cn

Antonio Hernández Daranas - *Instituto de Productos Naturales y Agrobiología. Consejo Superior de Investigaciones Científicas (IPNA-CSIC), La Laguna, 38206 Tenerife, Spain;* Email: adaranas@ipna.csic.es

Author Contributions

The manuscript was written through contributions of all authors. ‡S-W.L and C.C. contributed equally.

Song-Wei Li - *State Key Laboratory of Drug Research, Shanghai Institute of Materia Medica, Chinese Academy of Sciences, No. 555, Zu Chong Zhi Road, Zhangjiang Hi-Tech Park, Shanghai 201203, China; Nanjing University of Chinese Medicine, 138 Xianlin Road, Nanjing 210023, China*

Cristina Cuadrado - *Instituto de Productos Naturales y Agrobiología. Consejo Superior de Investigaciones Científicas (IPNA-CSIC), La Laguna, 38206 Tenerife, Spain*

Li-Gong Yao - *State Key Laboratory of Drug Research, Shanghai Institute of Materia Medica, Chinese Academy of Sciences, No. 555, Zu Chong Zhi Road, Zhangjiang Hi-Tech Park, Shanghai 201203, China*

Notes

The authors declare no competing financial interest.

ACKNOWLEDGMENT

We thank a reviewer for suggesting the comparative using the X-ray structures. This research work was financially supported by the Natural Science Foundation of China (No. 81991521), the Drug Innovation Major Project (No. 2018ZX09711-001-001-009). A.H.D thanks the CSIC for a JAE-intro grant to C.C.G. This study made use of the SGAI-CSIC supercomputing facilities. We thank M.H. Dorta for help with graphics edition and G. Jones, funded by Cabildo de Tenerife, TFinnova Programme supported by MEDI and FDCAN for English edition.

REFERENCES

(1) Carroll, A. R.; Copp, B. R.; Davis, R. A.; Keyzers, R. A.; Prinsep, M. R. *Nat. Prod. Rep.* **2020**, *37* (2), 175–223.
(2) Rodrigues, I. G.; Miguel, M. G.; Mnif, W. *Molecules* **2019**, *24* (4), 781.
(3) Borman, S. *C&EN Glob. Enterp.* **2017**, *95* (7), 7–7.
(4) *Modern NMR Approaches to the Structure Elucidation of Natural Products*; Williams, A., Martin, G., Rovnyak, D., Eds.; Royal Society of Chemistry, 2017.
(5) Chhetri, B. K.; Lavoie, S.; Sweeney-Jones, A. M.; Kubanek, J. *Nat. Prod. Rep.* **2018**, *35* (6), 514–531.
(6) Kutateladze, A. G.; Krenske, E. H.; Williams, C. M. *Angew. Chemie Int. Ed.* **2019**, *58* (21), 7107–7112.
(7) Kutateladze, A. G.; Holt, T. *J. Org. Chem.* **2019**, *84* (12), 8297–8299.
(8) Grimblat, N.; Kaufman, T. S.; Sarotti, A. M. *Org. Lett.* **2016**, *18* (24), 6420–6423.
(9) Ye, F.; Zhu, Z.-D.; Chen, J.-S.; Li, J.; Gu, Y.-C.; Zhu, W.-L.; Li, X.-W.; Guo, Y.-W. *Org. Lett.* **2017**, *19* (16), 4183–4186.
(10) Ye, F.; Li, J.; Wu, Y.; Zhu, Z.-D. Mollo, E.; Gavagnin, M.; Gu, Y.-C.; Zhu, W.-L.; Guo, Y.-W. *Org. Lett.* **2018**, *20* (9), 2637–2640.
(11) Li, G.; Li, H.; Zhang, Q.; Yang, M.; Gu, Y.-C.; Liang, L.-F.; Guo, Y.-W. *J. Org. Chem.* **2019**, *84* (9), 5091–5098
(12) Rahelivao, M. P.; Gruner, M.; Lübken, T.; Islamov, D.; Kataeva, O.; Andriamanantoanina, H.; Bauer, I.; Knölker, H. J. *Org. Biomol. Chem.* **2016**, *14* (3), 989–1001.
(13) Matsumori, N.; Kaneno, D.; Murata, M.; Nakamura, H.; Tachibana, K. *J. Org. Chem.* **1999**, *64* (3), 866–876.
(14) Domínguez, H. J.; Napolitano, J. G.; Fernández-Sánchez, M. T.; Cabrera-García, D.; Novelli, A.; Norte, M.; Fernández, J. J.; Daranas, A. H. *Org. Lett.* **2014**, *16* (17), 4546–4549.
(15) Cen-Pacheco, F.; Rodríguez, J.; Norte, M.; Fernández, J. J.; Hernández Daranas, A. *Chem. - A Eur. J.* **2013**, *19* (26), 8525–8532.
(16) Lodewyk, M. W.; Siebert, M. R.; Tantillo, D. J. *Chem. Rev.* **2012**, *112* (3), 1839–1862.
(17) Grimblat, N.; Sarotti, A. M. *Chem. - A Eur. J.* **2016**, *22* (35), 12246–12261.
(18) Bifulco, G.; Dambruoso, P.; Gomez-Paloma, L.; Riccio, R. *Chem. Rev.* **2007**, *107* (9), 3744–3779.
(19) Smith, S. G.; Goodman, J. M. *J. Am. Chem. Soc.* **2010**, *132* (37), 12946–12959.
(20) Ermanis, K.; Parkes, K. E. B.; Agback, T.; Goodman, J. M. *Org. Biomol. Chem.* **2017**, *15* (42), 8998–9007.
(21) Grimblat, N.; Zanardi, M. M.; Sarotti, A. M. *J. Org. Chem.* **2015**, *80* (24), 12526–12534.
(22) Grimblat, N.; Gavín, J. A.; Hernández Daranas, A.; Sarotti, A. M. *Org. Lett.* **2019**, *21* (11), 4003–4007.
(23) Lauro, G.; Das, P.; Riccio, R.; Reddy, D. S.; Bifulco, G. *J. Org. Chem.* **2020**, *85* (5), 3297–3306.
(24) Smith, S. G.; Goodman, J. M. *J. Org. Chem.* **2009**, *74* (12), 4597–4607.
(25) Willwacher, J.; Heggen, B.; Wirtz, C.; Thiel, W.; Fürstner, A. **2015**, 10416–10430.
(26) Kutateladze, A. G.; Mukhina, O. A. *J. Org. Chem.* **2014**, *79* (17), 8397–8406.
(27) Zanardi, M. M.; Marcarino, M. O.; Sarotti, A. M. *Org. Lett.* **2020**, *22* (1), 52–56.